5.1 Introduction

The main objective of nanotechnology is to understand and gather information of any materials at its molecular level for its utilization as nanoscopic sized electronic devices. Ultra-low concentration detection device fabrication for any molecule is being main aim of researchers from all over the world. The discovery of graphene, a two dimensional material was the major breakthrough for the development of nano detectors [1-3]. Graphene has extraordinary electronic and transport properties arising from sp^2 C-C bonding [4], and attention seeking extremely high surface-to-volume ratio which inspires researchers to explore other materials having similar hybridization in its two dimensional form. Till date hexagonal-boron nitride (h-BN), phosphorous, silicon, transition metal sulfides and many other materials have been predicted or synthesized in monolayer form [5-9]. Boron nitride nanostructures (BNNs) [5] have the closest structural analogy to carbon nanostructures. In boron nitride structure boron (group III) and nitrogen (group V) have equal contribution. Boron nitride has similar isomers just like carbon, in 3D it has cubic boron nitride (c-BN) which is similar to diamond, in 2D it has hexagonal boron nitride sheet (h-BN) which is analogous to graphene, in 1D it has boron nitride nanotube (BNNT) and boron nitride nanoribbon (BNNR) just as carbon nanotube (CNT) and graphene nanoribbon (GNR) [10]. The reason behind the superiority of BN nanostructure (BNNs) over graphene for utilization in sensors and nanoelectronics [11-12] is its semiconducting nature contrast to graphene.

Special attention is gathered by boron nitride nanoribbon (BNNR) among all BNNs, because of its exceptional optical properties, electronic, magnetic and thermal stability arising due to its edge structure and is better than graphene nanoribbon GNR [13]. Due to the nature of bonding between B-N it possess tremendously different properties

from GNR apart from its structural similarity with it. In BNNR every B atom in the hexagonal ring comprises its structure bonded with other three N atoms and vice versa, with strong directional bond which helps in the formation of planar structure for BNNR. The BNNR has π-orbital electron localized near N atom than the B atom, because B atom shares one to two electrons with its three neighbouring N atoms [14]. Zeng and co-workers successfully jumped the hurdle which was in the path for the fabrication of BNNR with the help of well-established arc plasma etching method which was previously utilized to make GNR from CNT [15]. The major drawback of above method was lack in the formation of high aspect ratio ribbons which was overcome by Erickson et al. [16] who developed an efficient process to fabricate high aspect ratio BNNRs from BNNT. Similar to the structure of GNR, BNNR can have armchair (A), zigzag (Z) and chiral (C) edges morphology but exceptional electronic and magnetic properties, arises due to its hydrogen passivated edges [17-18]. Qi et al. [19] developed a method which is able to tune the electronic properties of BNNR for its utilization in opto-electronic devices, photovoltaic, electronic and piezoelectric devices. They also revealed the distinct physics of BNNR which is totally different from GNRs. The effect of strain on the electronic properties is also analyzed in this work. The capability to tune the properties of BNNR makes it superior than GNR and a suitable nanomaterial for the applications in bio sensing.

Neurological imbalance of neurotransmitters is the major reason for many health issues. The main responsible chemical for any signal transmission between neuron cells is the neurotransmitters [20]. The main work of neurotransmitter in our nervous system is to work as a chemical messenger to pass the information by exciting near neuron or the targeted tissue [21]. One of the most important type of neurotransmitters is monoamines, which contains adrenaline, dopamine (DA), histamine, melatonin, noradrenaline and

serotonin [22]. From the name itself it is self-explanatory that it contains one amino group having aromatic ring which further connected with two carbon chain (–CH 2 –CH 2 –) which can act as both neurotransmitters and neuromodulators. Dopamine (DA) and Adrenaline (AD) are of significant importance among all neurotransmitters.

Dopamine (DA) basically belongs to phenethylamine and catecholamine families which plays a significant role in several brain and body functions. DA is synthesized in the kidneys and brain by a chemical precursor L-DOPA, in which carboxyl group is removed. The DA release helps to motivate behaviour which is released in the brain as a reward mechanism. The formation of DA can be increased by different ways in brain but worst is addiction of drugs, because drugs intake is one of the methods used to boost its amount. Many serious neurological disorders arise due to abnormal production of DA. Many deceases arise due to insufficient production of DA in brain like restless leg syndrome and schizophrenia, attention deficit hyperactive disorder, Parkinson's disease and HIV infections [23-26]. Adrenaline (AD) or epinephrine is another important neurotransmitter which plays a significant role in the nervous system of all mammals. It helps to control variety of physiological process and behaviour with different receptors. Both of these neurotransmitters are very essential in the body and their imbalance entwines many diseases in humans. To monitor and measure these molecules there have been intense efforts by many researchers from many years to develop improved and efficient sensors [12, 27, 28-36].

The method for determination and detection of neurotransmitters is very expensive and also environmental sensitive [37-41]. That’s why it is very challenging to monitor or detect these molecules and requires a highly sensitive and simple method which can be achieve with the help of electrochemical sensors [37]. There exist many theoretical and

experimental studies for the development of sensitive electrochemical sensors for neurotransmitters using nanomaterials [42-45]. The nanoscopic electronic devices can be developed through understanding the molecular level information, which is the main aim in advancement of nanotechnology. In a recent study done with graphene (doped and defected) by Ortiz-Medina et al. [42] reports it to be used as a DA sensor and also check the effect of electric field on the sensitivity of graphene towards DA. Feng et al. [43] developed a 3D N-doped graphene porous foam for sensing dopamine while Fernández et al. [44] reported that the pristine and defected graphene interacting non-covalently with DA. Systematic study done by Khan [45] to check the sensing ability of 2D h-BN with different surfactant towards DA concludes its improved sensing ability. From the literature it was clear that there are many studies reported on DA sensor but to the best of our knowledge no report exists on adrenaline sensor. There is no study focussing on boron nitride nanostructures mainly BNNR for its utilization as sensor for DA and AD. The main motivation for this study is lack of molecular level understanding of sensors for dopamine and adrenaline which inspired us to explore BNNRs as a possible neurotransmitter sensor. The present work focuses on the understanding of adsorption mechanism between BNNR and two different neurotransmitters (dopamine and adrenaline) along with the geometrical effect of BNNRs (ABNNR and ZBNNR) on adsorption.

5.2 Computational Methods

The first principle calculations have been performed under the framework of density functional theory (DFT) for the present study using Quantum Espresso (QE) simulation package [46]. The ultrasoft (US) Rappe Rabe Kaxiras Joannopoulos (RRKJ) pseudopotential using Broyden-Fletcher-Goldfarb-Shanno (BFGS) [47] method with suitable generalized gradient approximation (GGA) as exchange-correlation functional has

been utilized [48]. To obtain a good convergence for single particle functions plane wave basis set we used 60 Ry and 600 Ry value for kinetic energy and charge density cut offs respectively. For the better evaluation of adsorption and electronic properties we have used uniform Monkhorst and Pack [49] k-point grids of size 1x1x16 in Brillouin zone (BZ). This k-point mesh guaranteed any violation of charge neutrality which is adequate for the convergence of all calculations. The bond length between boron and nitrogen of pristine BNNR is 1.45 Å in the ground state configuration. The integration of both neurotransmitters (adrenaline and dopamine) with zigzag and armchair chirality BNNR has been comparatively analysed by full structural optimization, adsorption energy, electronic band structure calculations and work function. Accounting the dispersion forces is necessary for studying adsorption of a molecule on a nanosurface is important [50-52]. Therefore, we have selected an appropriate method which is capable to correctly consider the long range electron correlation. Grimme's dispersion correction (DFT-D2) [53] is used in the present study because it is reported that the non-covalent long distance van der Waals interaction calculated by DFT-D2 is comparable with DFT-D3 [54]. The adsorption energy E_{ad} for neurotransmitters over BNNRs has been calculated according to the following equation:

$$E_{ad} = E_{BNNRs + neurotransmitter} - (E_{BNNRs} + E_{neurotransmitter}) \quad (5.1)$$

Where $E_{BNNRs + neurotransmitter}$ is the total energy of BNNRs adsorbed by neurotransmitter (adrenaline (AD) and dopamine (DA)), E_{BNNRs} is the total energy of the adsorbent nanoribbon, $E_{neurotransmitter}$ is the total energy of neurotransmitter (AD and DA) obtained from their full optimized geometries. Further, with the help of Gaussian 09 suite of package [55-56], the highest occupied molecular orbitals (HOMO) and lowest unoccupied molecular orbitals (LUMO) of dopamine and adrenaline are calculated with HSE06 level

using 6-31+G(D) basis set. Single point calculations are performed at the same level of theory for accurate prediction of HOMO and LUMO. The geometrical structures of both neurotransmitters are in true minima after optimization as there is no imaginary frequency.

5.3 Results and Discussion

To develop better understanding for the interaction between neurotransmitter (dopamine and adrenaline) and boron nitride nanoribbons (ABNNR and ZBNNR) these are first individually optimized. The individual optimized structure of dopamine, adrenaline, ABBNR and ZBNNR is presented in Figs. 5.1 (a-d). Both BNNRs, are periodic in z-axis and therefore multiplied in z-direction. The supercell of 1x1x4 of ABNNR and 1x1x7 of ZBNNR with 88 and 84 atoms, respectively provides large surface for molecules to interact. The width of the ABNNR and ZBNNR is 12 Å and 11.5 Å, respectively after optimization. The structure of both neurotransmitters having an aromatic ring with the attachment of two oxygen. Additionally, in the structure of an adrenaline molecule one can observed the presence of an extra oxygen atom and a methyl group compared to dopamine. Figs. 5.2 (a-b) and Figs. 5.3(a-b) show the optimized structure of dopamine and adrenaline adsorbed over BNNRs, respectively. After the adsorption, the distance between dopamine over ABNNR and ZBNNR is 2.52 Å and 2.38 Å, respectively. On the other hand, we observed the 2.78 Å and 2.42 Å distance between adrenaline and ABNNR and ZBNNR, respectively (See Figs 5.2-5.3 and Table 5.2). Initially, the parallel orientation for both neurotransmitters is considered for the adsorption over BNNRs, as planar molecules prefer to adsorbed parallel compared to other orientations [51, 57-58].

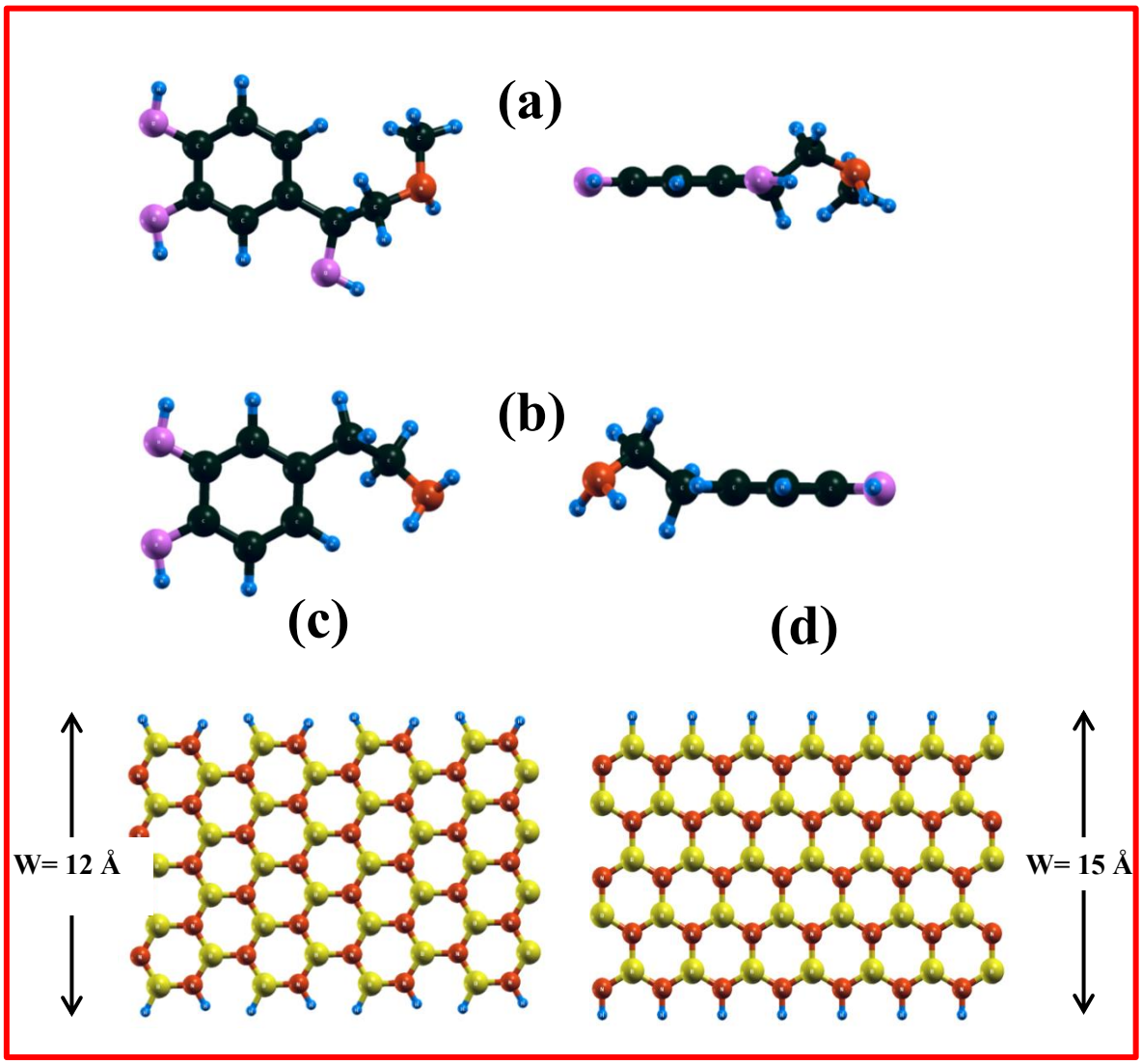

Figure 5.1: *Optimized structure of (a) adrenaline (b) dopamine (c) ABNNR and (d) ZBNNR. Oxygen, carbon, hydrogen boron and nitrogen are represented as pink, black, blue, yellow and orange ball respectively. W shows the width of both nanoribbons.*

After the adsorption of molecules, we observed the generation of bow on the surface of both BNNRs with the significant change in the bond length between the boron and nitrogen atom. Table 5.1 represents the change in the bond length along with the bond angle which gives clear indication of the interaction of molecules with BNNRs.

Table 5.1: *Calculated Bond length (Å) and Bond angle (º) between B-N-B in BNNRs.*

Bond lengths	Pristine (Å)	After adsorption (Å)
39N-34B	1.450	1.448
39N-54B	1.452	1.455
56N-50B	1.449	1.447
28B-29N	1.449	1.451
55N-56B	1.451	1.453
28B-13N	1.450	1.454
30B-29N	1.451	1.459

Bond angles	Pristine (º)	After adsorption (º)
54B-39N-34B	120	120.114
34B-33N-32B	120	120.106
35N-30B-29N	119.95	120.241
38B-39N-34B	119.86	119.578
13N-28B-33N	120.13	120.450

Our study confirms the physisorption of neurotransmitters with the BNNRs and also the absence of any covalent bond as we observed a large distance between BNNRs and molecules after the optimization. An adsorption energetics of adsorbate with adsorbent plays an important role in describing the magnitude and nature of interaction; and also helpful in predicting whether the molecule is interacting with the surface or not. To calculate the adsorption energy for DA and AD over both ABNNR and ZBNNR, we have used equation (5.1). Adrenaline is strongly physisorbed over ABNNR with the E_{ad} = -1.144 eV adsorption energy compared to dopamine (E_{ad} = -1.013 eV, adsorption distance of 2.52 Å with ABNNR) with the adsorption distance of 2.38 Å.

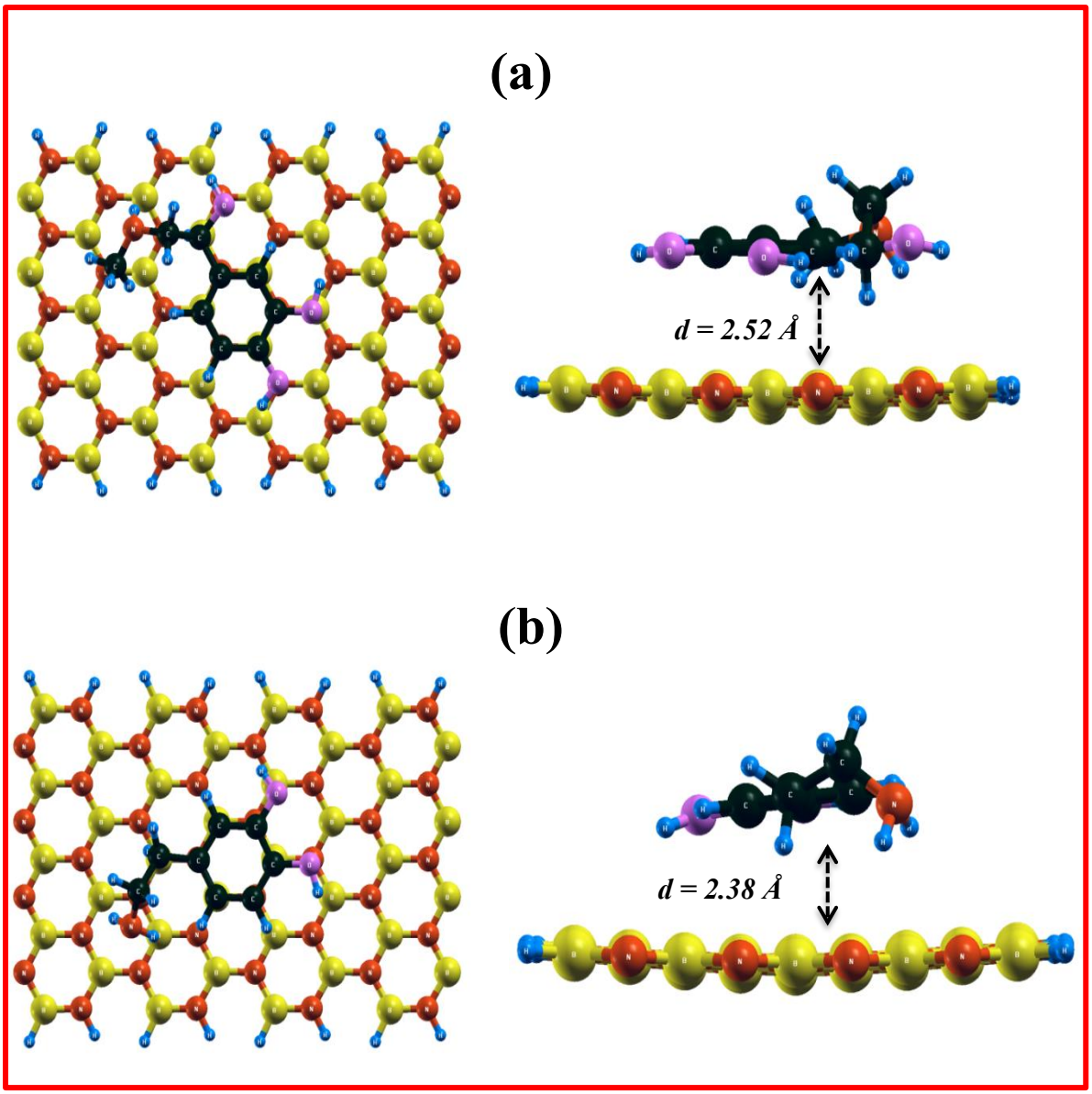

Figure 5.2: *Optimized structure of ABNNR adsorbed with (a) adrenaline and (b) dopamine. The distance between the molecules and BNNRs, is represented by d.*

We observed similar trend for the adsorption of DA (E_{ad} = -0.701 eV, adsorption distance of 2.78 Å) and AD (E_{ad} = -0.824 eV, adsorption distance of 2.42 Å) over ZBNNR. The presence of an extra oxygen atom in the adrenaline making it more electronegative than the dopamine as it is attributed to the difference in the adsorption energy.

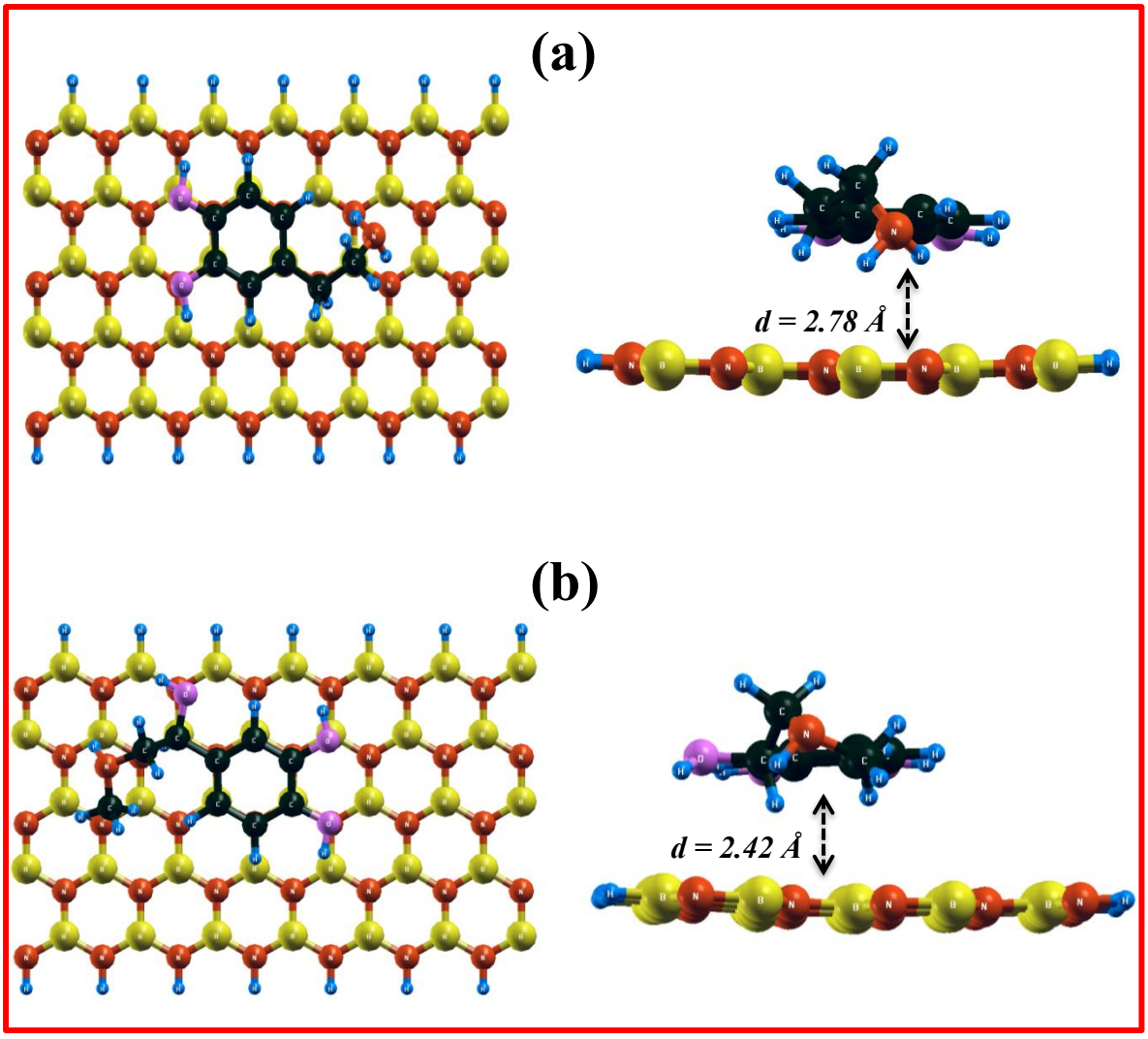

Figure 5.3: *Optimized structure of ZBNNR adsorbed with (a) dopamine and (b) adrenaline. The distance between the molecules and BNNRs, is represented by d.*

The higher sensitive semiconducting nature of ABNNR towards the flow of any external charge is the reason for making the strong interaction with neurotransmitters (DA and AD) compared to ZBNNR [59]. The inclusion of van der Waals interaction is helpful to develop insight in to calculated adsorption energy difference which is influenced by the size and mass of any molecule and chirality of ribbons [60]. The calculated non-covalent adsorption energy is considerably higher compared to graphene [44]. Fernandez et al. [44] have studied the adsorption interaction of dopamine over graphene using different

functionals and observed adsorption energy in the range of +0.20 to -0.94 eV which is relatively lower than our study.

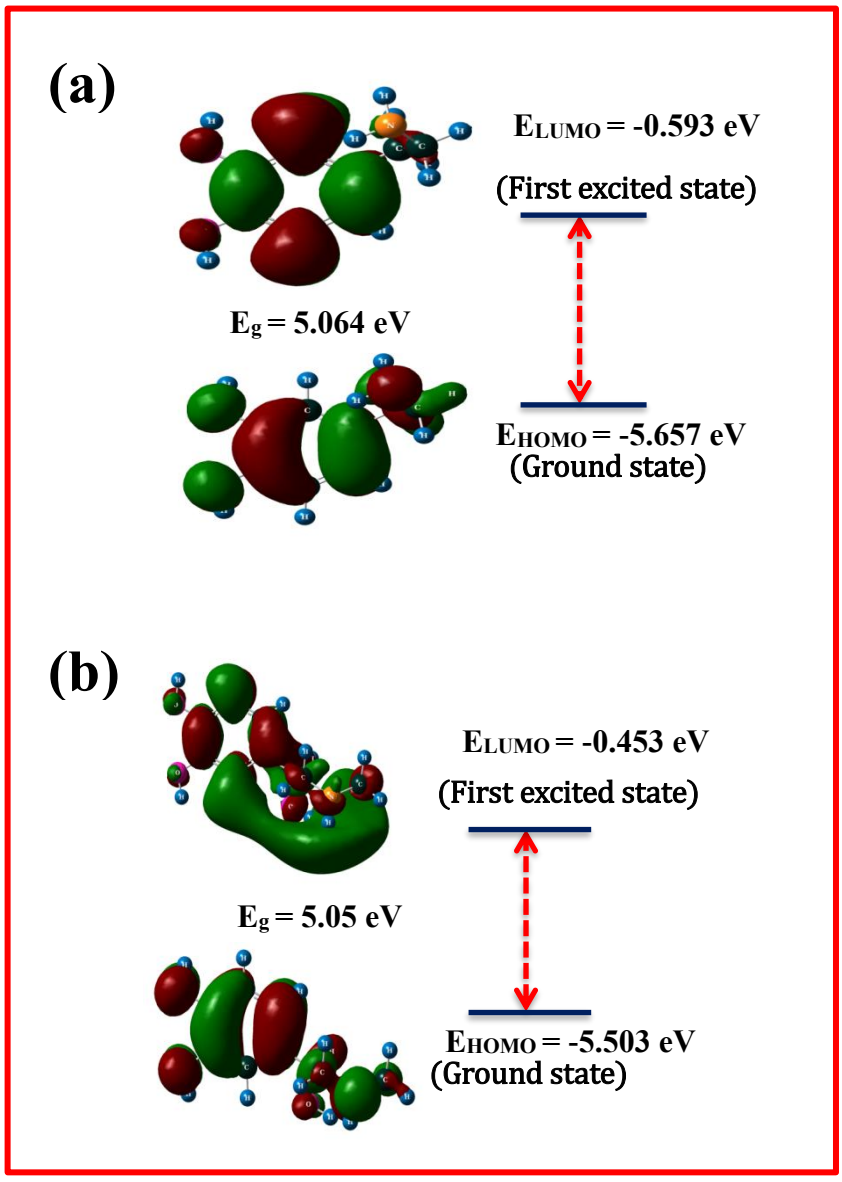

Figure 5.4: *Molecular orbitals of (a) dopamine and (b) adrenaline.*

Though, our result of adsorption energy of dopamine is comparable with the study of adsorbed dopamine over defected graphene. Urdaneta et al. [61] found that the dopamine binds covalently and chemisorbed over the TiO_2 surface which is in contrast to our study. The big drawback of chemisorbed molecules is that they require more energy to

release than the physisorbed molecules for drug delivery, therefore in most cases physisorption is preferred for better drug delivery system. Due to non-covalent interaction with both molecules, BNNRs are more preferable for the drug release and delivery. The nature of interaction between adsorbate and adsorbent offers benefits in terms of easy reusability and removal of nanostructure without perturbing the structural and electronic change of the considered system.

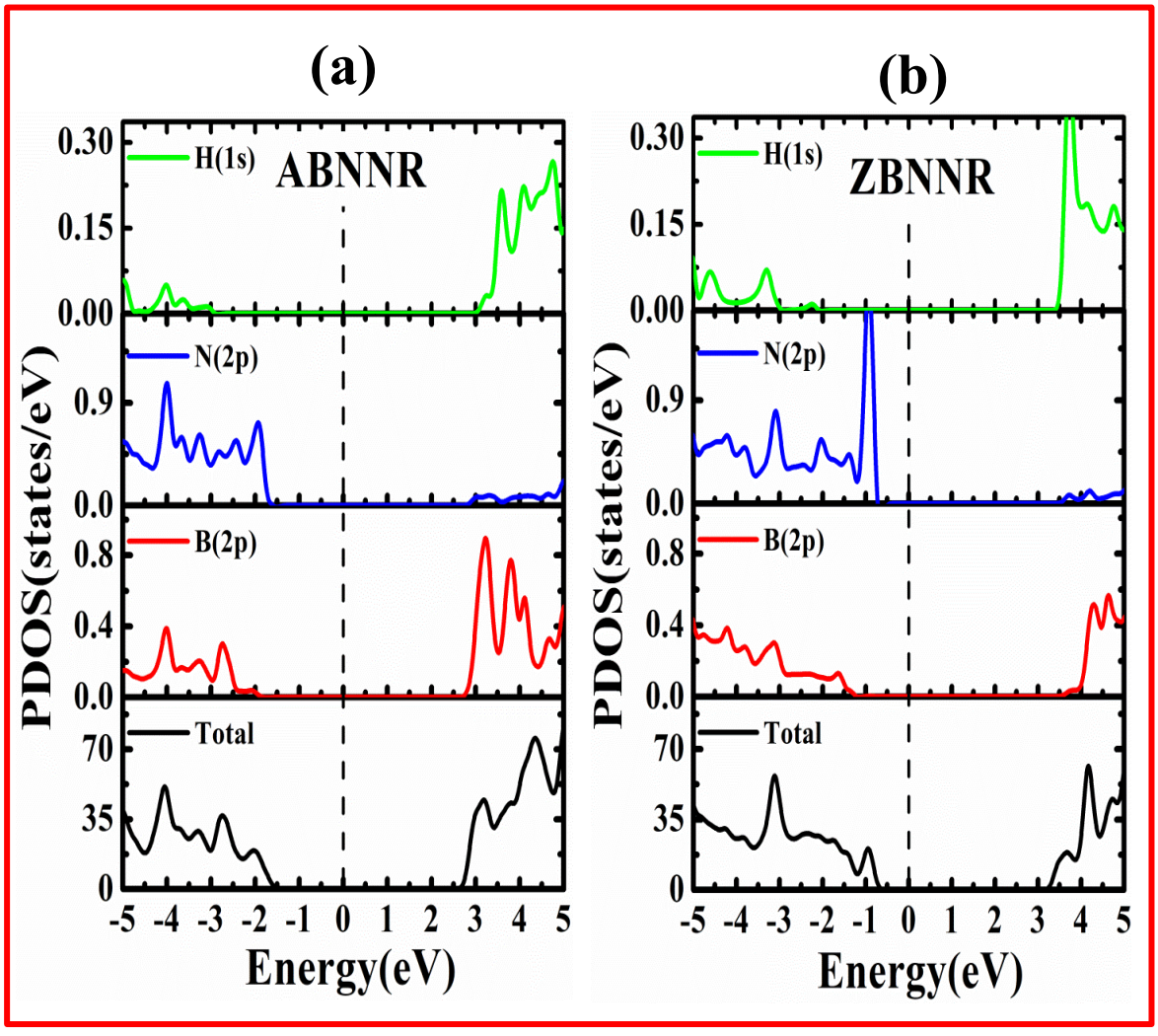

Figure 5.5: *Total and partial DOS of (a) ABNNR and (b) ZBNNR.*

The molecular orbitals of both neurotransmitters are presented in Figs. 5.4 (a-b). The calculated HOMO-LUMO gap for DA and AD molecules is 5.064 eV and 5.05 eV

respectively. As can be seen from Figs. 5.4(a-b) the HOMO wave functions are distributed over whole molecule for both the DA and AD molecules. The HOMO of DA displays the existence of p-orbitals on catechol ring along with hydroxyl groups which makes the amine group of dopamine less reactive. The resulting slight bow structure of both ABNNR and ZBNNR is attributed to the significantly attractive p-orbitals.

***Table 5.2**: Calculated energy gap (E_g), difference in band gap (ΔE_g), adsorption energy (E_{ad}), distance between neurotransmitter and BNNRs, Fermi energy (E_F) and work function (Φ.)All values are in eV.*

System	ABNNR			ZBNNR		
	Pristine	DA	AD	Pristine	DA	AD
E_g(eV)	4.163	3.171	3.028	3.842	3.073	2.900
ΔE_g (eV)	-	0.992	1.135	-	0.769	0.942
E_{ad} (eV)	-	-1.013	-1.144	-	-0.701	-0.824
d (Å)	-	2.52	2.38	-	2.78	2.42
E_F	-3.061	-1.807	-1.826	-3.902	-2.083	-2.355
Φ (eV)	4.152	3.057	3.111	4.970	3.350	3.661

Fig. 4(a) clearly shows the undistinguishable hydroxyl group in the LUMO of dopamine encloses strong p-orbitals. Likewise, the HOMO exists almost all over the catechol ring and nitrogen atom for the AD. On the contrary, the LUMO is spread over the carbon chain for AD. The calculated total density of states (DOS) and partial density of states (PDOS) of pristine BNNRs (ABNNR and ZBNNR) are plotted in Figs. 5.5(a-b). The plots of electronic structure clearly depict the wide bandgap semiconducting nature of BNNRs with the band gap of 4.163 eV (ABNNR) and 3.842 eV (ZBNNR).

The calculated energy gap (E_g), adsorption energy (E_{ad}), Fermi energy (E_f) and distance of the adsorbed molecules of BNNRs are presented in Table 5.2. In case of ABNNR, major contribution of 2p orbital of nitrogen atom can be seen in valence band region within the range between -2 to -10 eV, with the small contribution of 1s orbital of hydrogen and 2p orbital of boron. The contribution of 2p orbital is distributed in two regions one in the conduction band [2 to 6 eV] and another one in the lower valence band region near -16 to -20 eV. Similar, trend is observed for the contribution of orbitals in the density by nitrogen and boron in case of ZBNNR. Furthermore, we have calculated DOS

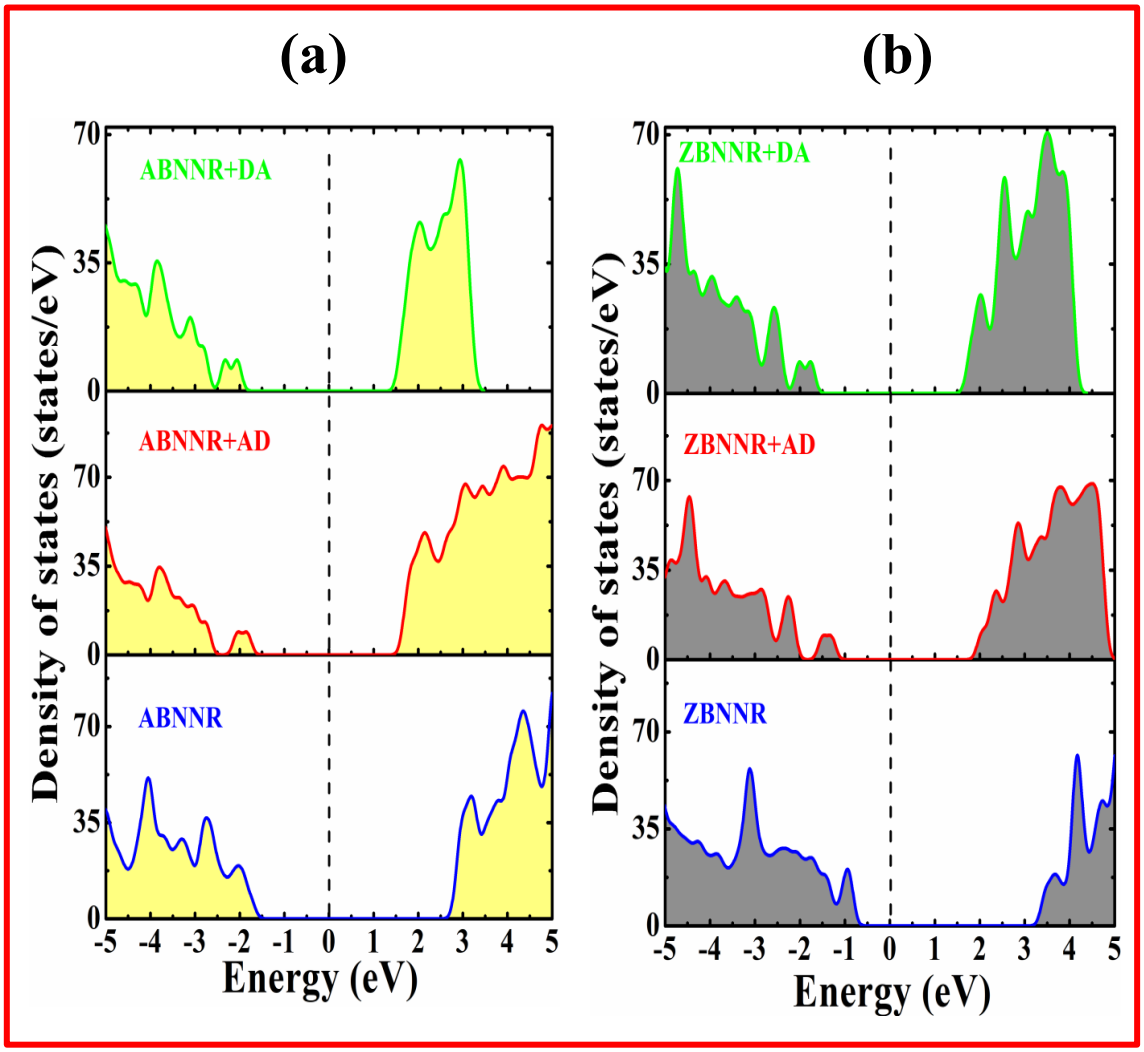

Figure 5.6: *Density of states of (a) ABNNR adsorbed neurotransmitter and (b) ZBNNR adsorbed neurotransmitter.*

for neurotransmitter over BNNRs system to develop more understanding with respect to electronic structure of pristine BNNRs (See Figs 5.6(a-b)).

The generation of some impurity states are responsible for the modification in the electronic properties due to the adsorption of DA and AD molecules over both BNNRs. The reduced bandgap is observed after the adsorption of neurotransmitters over BNNRs; reduction in the bandgap by AD is more noticeable compared to DA for both BNNRs. The reason behind the large reduction in bandgap compared to DA can be attributed to the presence of an extra oxygen atom in the configuration of AD.

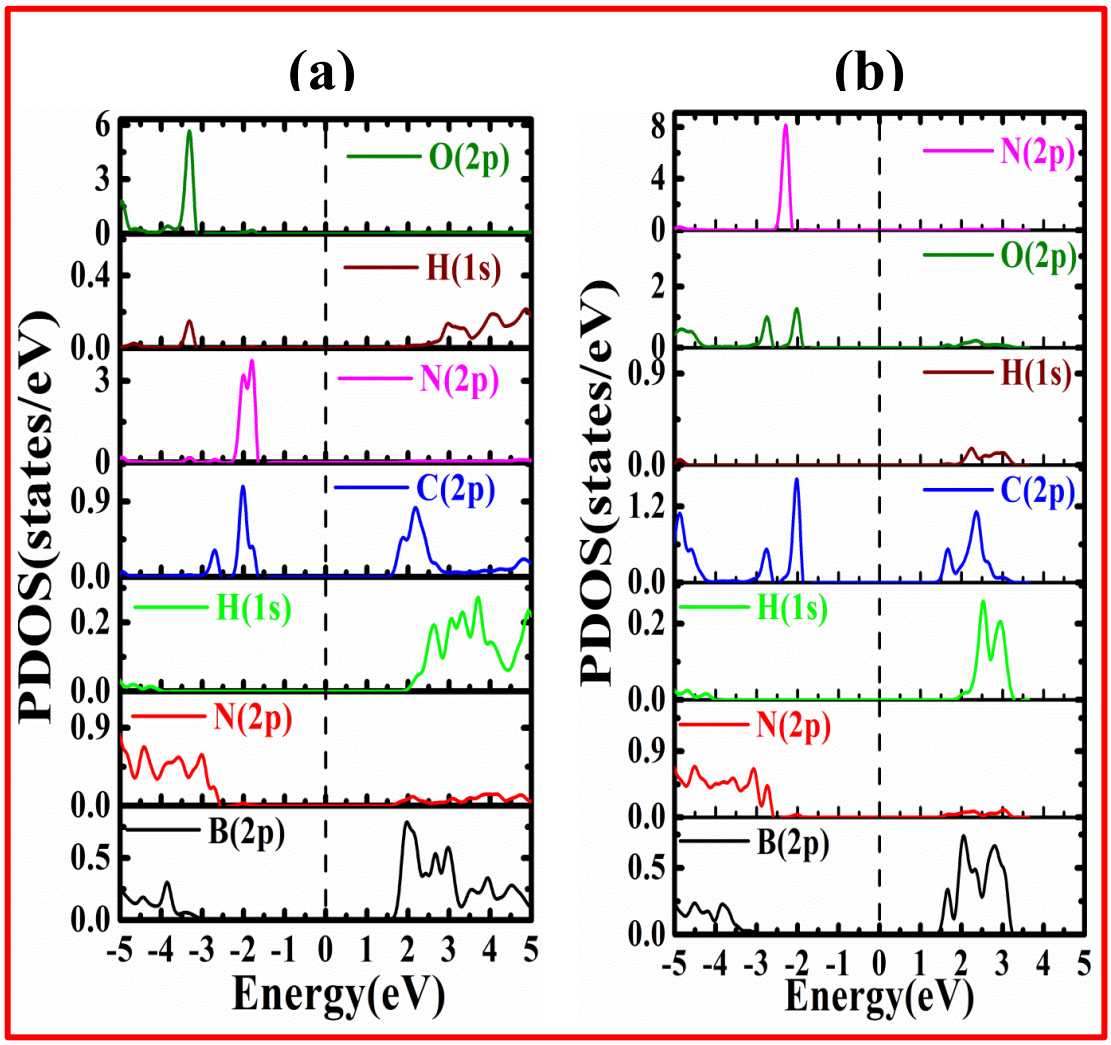

Figure 5.7: *Partial density of states of ABNNR adsorbed with (a) Adrenaline and (b) Dopamine.*

To develop a systematic insight of the modification of the electronic properties of BNNRs by neurotransmitter, we presented the PDOS for all systems in Figs. 5.7 and 5.8. From the PDOS, one can clearly see the impact of both DA and AD molecules confined at top and middle of the valence band.

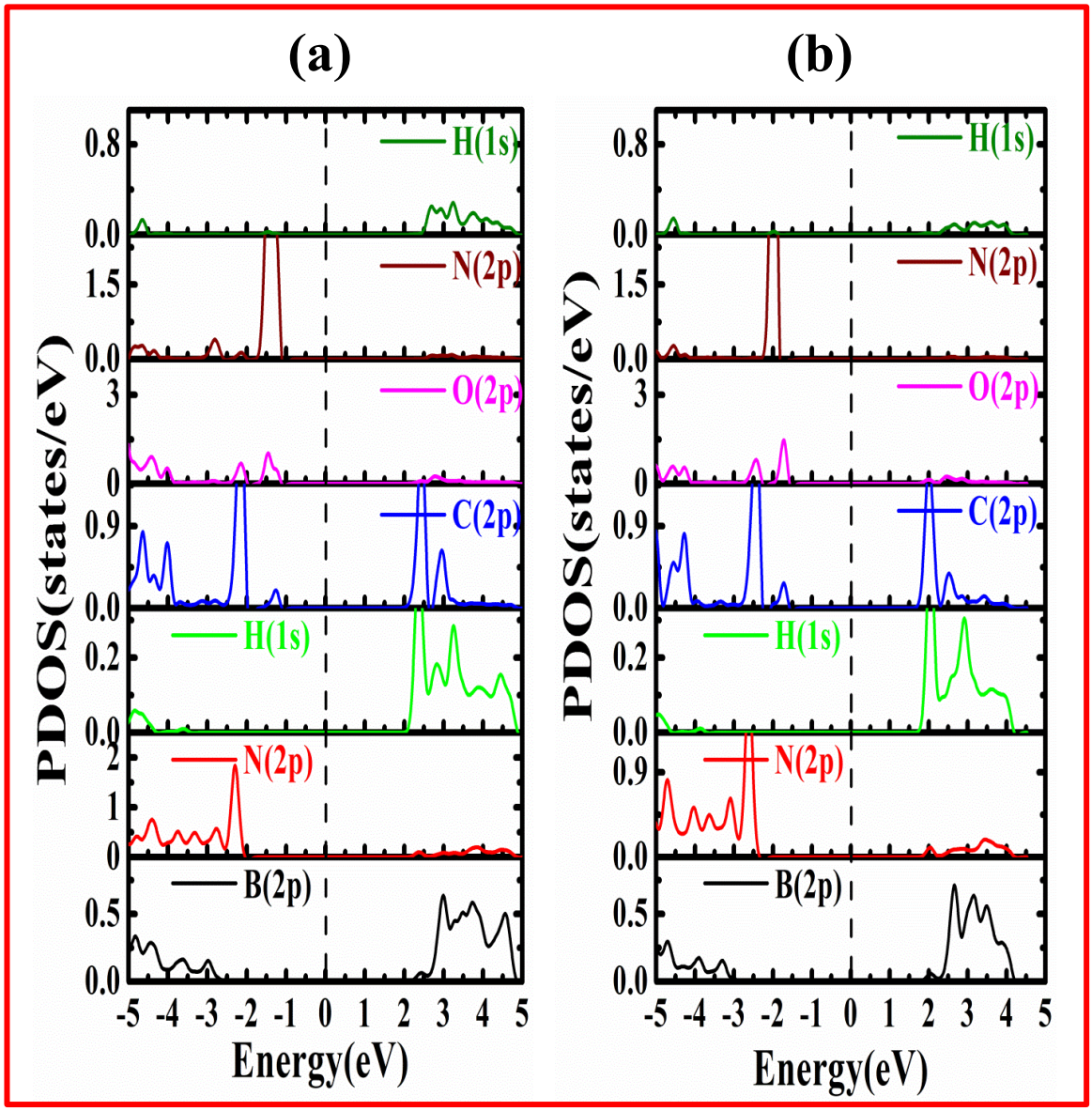

Figure 5.8: *Partial density of states of ZBNNR adsorbed with (a) Adrenaline and (b) Dopamine.*

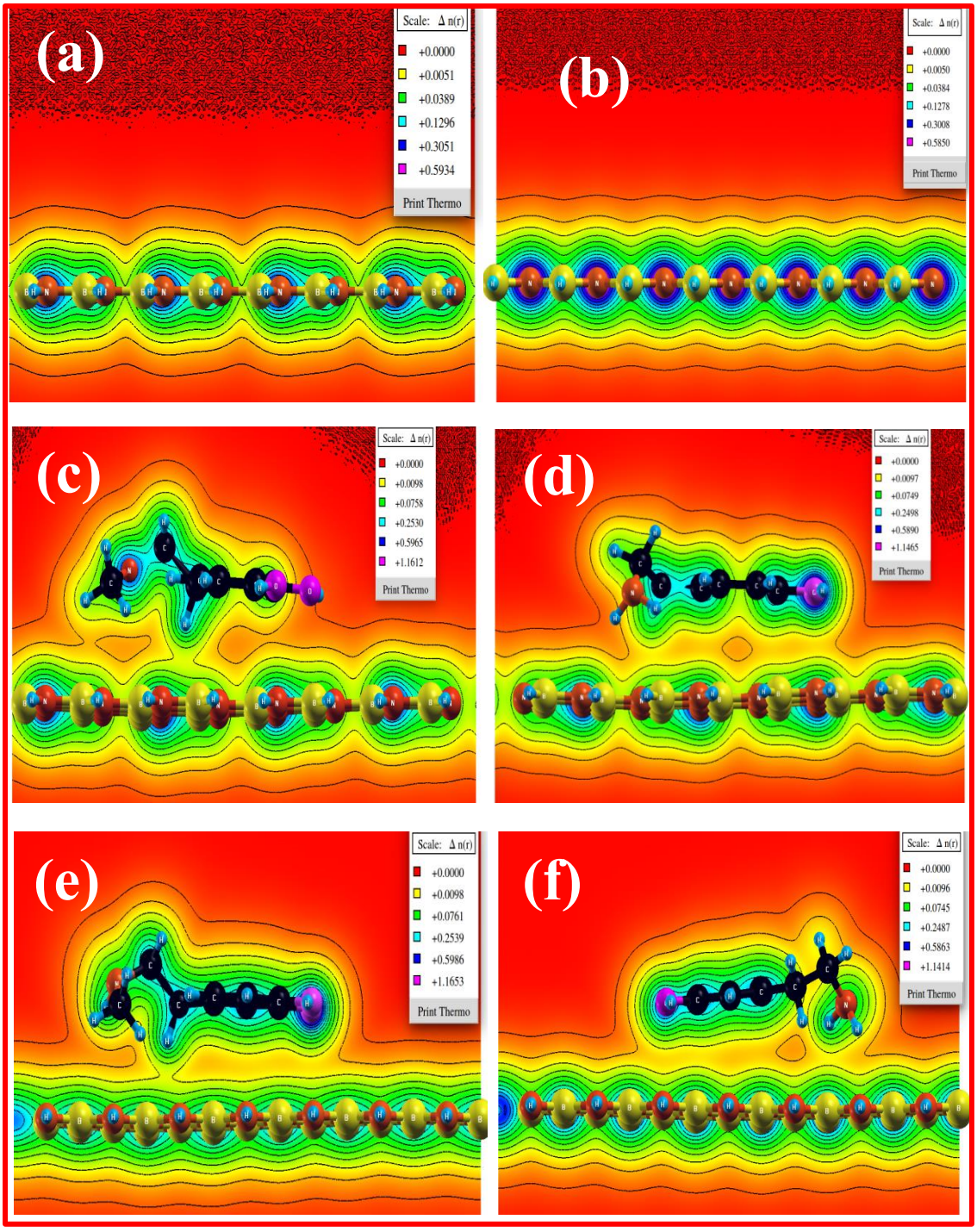

Figure 5.9: *Charge density plots (a-b) ABNNR/ZBNNR, (c-d) DA adsorbed ABNNR and AD adsorbed ABNNR and (e-f) DA adsorbed ZBNNR and AD adsorbed ZBNNR.*

For ABNNR, the p-orbital of carbon and nitrogen atoms present in AD causes states near the Fermi level in the valence band region where as in case of DA, states generated are as a result of carbon, nitrogen and oxygen. The impurity states in lower valence band are

led by 2p orbitals of carbon and nitrogen in AD/ABNNR, however, in DA/ABNNR system lower conduction band is contributed by the carbon and oxygen atom's 2p orbitals. From the PDOS plots of AD/ZBNNR and DA/ZBNNR, it is clearly seen that the impurity states arise after the adsorption as a consequence of 2p states of carbon, nitrogen and oxygen atoms.

Therefore, neurotransmitters seem to be an active unit which significantly affects electronic structure along with electron mobility upon adsorption over BNNRs. After adsorption of DA and AD, the bandgap of ABNNR decreases by the amount of 0.992 eV and 1.135 eV, respectively. Correspondingly, in ZBNNR the reduction in the band gap observed by DA is 0.769 eV and 0.942 eV for AD. The existence of an extra OH group in AD molecule is responsible for the large bandgap modulation of ABNNR which is absent in DA.

Our data strengthen the fact about physorption of molecules over nanosurface of both BNNRs, which gives strong indication about their suitability for the targeted delivery and due to its physisorption nature, reversibility of the nanoribbon can be simply accomplish by the desorption. By calculating the Lowdin charge transfer we analyzed the electron transport properties of systems. The significant charge transfer between the neurotransmitter (DA and AD) and both BNNRs, after the adsorption process is the reason for the variation in geometrical and electronic properties of BNNRs. The 0.10e and 0.15e charge transfer observed in the case of DA and AD respectively adsorbed over ABNNR, respectively while 0.10e and 0.12e charge transfer is observed for DA and AD respectively adsorbed over ZBNNR. The calculated charge density counter is shown in the Fig. 5.9.

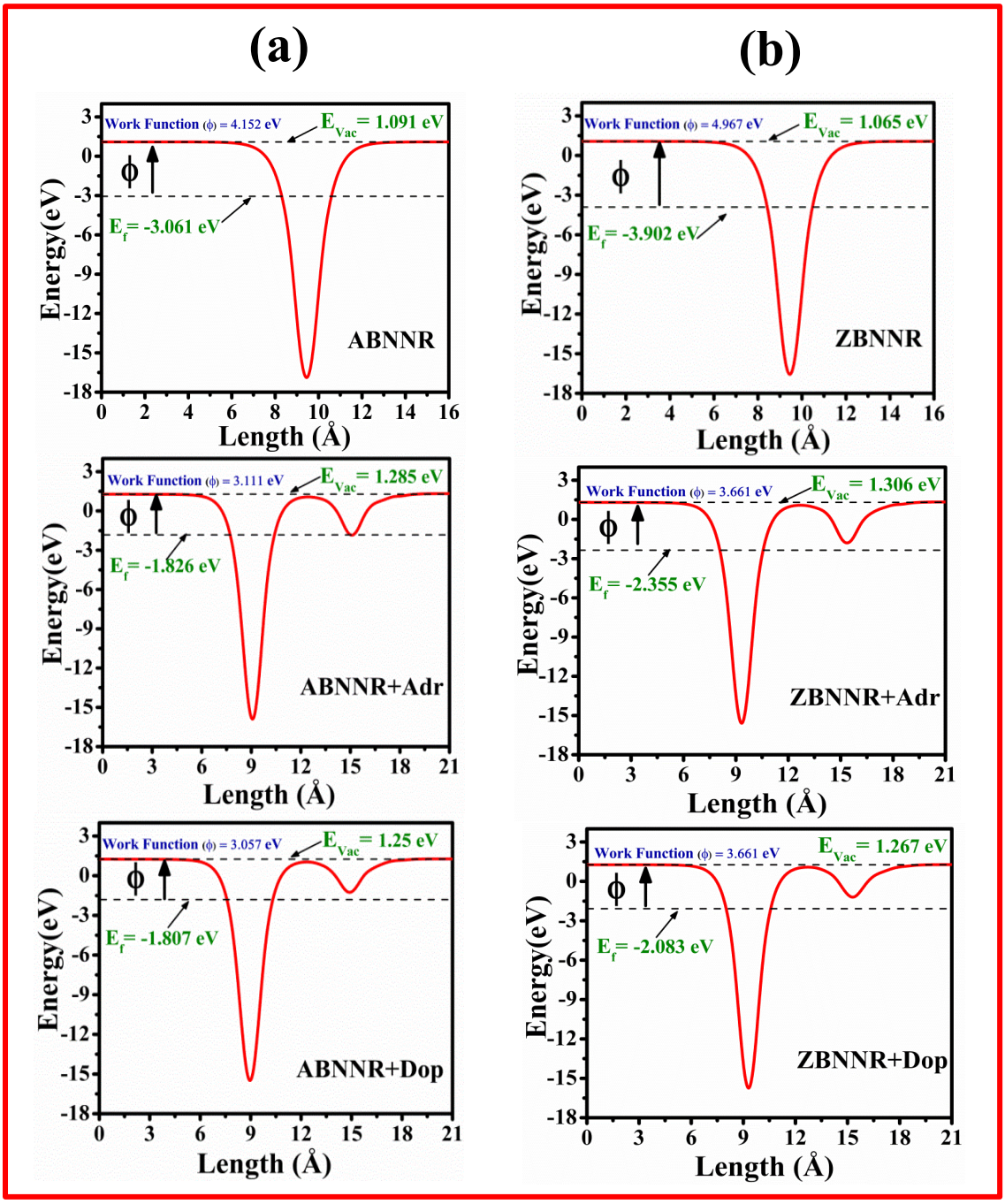

Figure 5.10: *Work function of BNNR and neurotransmitter adsorbed (a) ABNNR and (b) ZBNNR.*

The electrical conductivity (σ) is an important electronic parameter of a material (surface) to understand the changes in the electronic property after adsorption and can be evaluated by the energy gap E_g. The following classic expression can be used to evaluate electrical conductivity [62];

$$\sigma \propto e^{-E_g/2KT} \quad (5.2)$$

where K and T both are the Boltzmann's constant and temperature, respectively. One can clearly see from the Eqn. 5.2, that the conductivity is inversely proportional to the bandgap, which means higher is the electrical conductivity smaller the value of bandgap E_g at given temperature T. Consequently, adsorption of neurotransmitters over both BNNRs surface is responsible for the significantly decrement in the band gap which automatically increases the electrical conductivity σ of the BNNRs. The electrical conductivity enhancement in both ABNNR and ZBNNR is higher for AD compared to DA. An electrical signal arises because of the change in the Fermi level of BNNRs due to the neurotransmitters, hence it could be a potential candidate for the biosensor applications.

To shed light on the modification of the electronic properties of BNNRs by the adsorption of neurotransmitters (DA and AD), the work function can be useful; which we have calculated using first principles calculations [9, 62].

The so-called work function is the amount of energy required to spill over the electron from Fermi level of any material to the vacuum level and can be calculated using the expression given below [62]:

$$WF(\Phi) = E_{vac} - E_F \quad (5.3)$$

Where, E_{vac} represents the energy of vacuum level and E_F designates the energy of Fermi level. Figs. 5.10 (a-b) represent the calculated work function for considered systems. The position of the peak in plots can be useful to understand the distance of the molecule from the surface.

A dramatic change in the work function is observed after the adsorption of neurotransmitter over BNNRs. The 32% and 26% reduction in work function is observed after the adsorption of DA and AD over ZBNNR whereas 26% and 25% reduction in work

function is identified for the adsorbed DA and AD over ABNNR. The strong influence of these molecules on the BNNRs surface is confirmed by the distinct alternation of work function, WF (Φ) after the adsorption of DA and AD.

5.4 Conclusions

In summary, we adopted density functional theory calculations to investigate the adsorption of two seemingly important neurotransmitters dopamine and adrenaline over armchair and zigzag boron nitride nanoribbons. Our study depicted the role of boron nitride nanoribbons as a biosensor. The adsorption energetics and structural analysis demonstrated the physisorption of both dopamine and adrenaline over ABNNR and ZBNNR. We found that the planar BNNRs transformed into the slight arched structure after functionalized with both neurotransmitters. By comparing our study of neurotransmitters over BNNRs, we observed strong non-covalent interaction of dopamine and adrenaline with ABNNR compared to previous works and the reason for its semiconducting behaviour. From this study, our biggest hope for the future is actually from experimental community as experimental neurotransmitter carrier is yet to be developed. We hope that our study brings out the likelihood of BNNR in using it as carrier for dopamine and adrenaline and directed researchers to develop and access the viability of BNNR based biosensor and drug delivery system for neurotransmitter carrier.

References

1. A. K. Geim and K. S. Novoselov, *Nat. Mater.* **6**, 183 (2007).
2. K. S. Novoselov, A. K. Geim, S. V. Morozov, D. Jiang, M. I. Katsnelson, I. V. Grigorieva, S. V. Dubonos and A. A. Firsov, *Nature*, **438**, 197 (2005).

3. K. S. Novoselov, A. K. Geim, S. V Morozov, D. Jiang, Y. Zhang, S. V Dubonos, I. V Grigorieva and A. A. Firsov, *Science*, **306**, 666 (2004).
4. R. A. Potyrailo, C. Surman, N. Nagraj and A. Burns, *Chem. Rev.*, **111**, 7315 (2011).
5. X. Song, J. Hu and H. Zeng, *J. Mater. Chem. C*, **1**, 2952 (2013).
6. A. L. M. T. Costa, F. W. N. S. and E. B. B. *Semicond. Sci. Technol*. **33**, 075018 (2018).
7. H. Liu, A. T. Neal, Z. Zhu, Z. Luo, X. Xu,, D. Toma´nek, and P. D. Ye, *ACS Nano*, **8**, 4033 (2014).
8. S. Cahangirov, M. Topsakal, E. Aktürk, H. Şahin, and S. Ciraci, *Phys. Rev. Lett.*, **102**, 236804 (2009).
9. K. Patel, B. Roondhe, S. D. Dabhi, P. K. Jha, *J. Hazard. Mater*. **351**, 337 (2018).
10. A. Rubio, J. L. Corkill and M. L. Cohen, *Phys. Rev. B*, **49**, 5081 (1994).
11. P. Singla, M. Riyaz, S. Singhal and N. Goal, *Phys. Chem. Chem. Phys.* **18**, 5597 (2016).
12. N. Saghayimarouf,, M. Monajjemi, *J. Comput. Theor. Nanosci.* **14**, 957 (2017).
13. M. Topsakal, E. Akturk and S. Ciraci, *Phys. Rev. B*, **79**, 115442 (2009).
14. Y. Muramatsu, T. Kaneyoshi, E. M. Gullikson and R. C. C. Perera, *Spectrochim. Acta – Part A Mol. Biomol. Spectrosc.*, **59**, 1951 (2003).
15. H. Zeng, C. Zhi, Z. Zhang, X. Wei, X. Wang, W. Guo, Y. Bando and D. Golberg, *Nano Lett.*, **10**, 5049 (2010).
16. K. J. Erickson, A. L. Gibb, A. Sinitskii, M. Rousseas, N. Alem, J. M. Tour and A. K. Zettl, *Nano Lett.*, **11**, 3221 (2011).
17. F. Zheng, G. Zhou, Z. Liu, J. Wu, W. Duan, B. L. Gu and S. B. Zhang, *Phys. Rev. B*, **78**, 205415 (2008).
18. L. Lin, L. Jing, W. Lu, L. Guangfu, Z. Jing, Q. Rui, G. Zhengxiang and N. M. Wai, *J. Phys. Chem. C*, **113**, 2273 (2009).
19. J. Qi, X. Qian, L. Qi, J. Feng, D. Shi and J. Li, *Nano Lett.*, **12**, 1224 (2012).
20. K. Jackowska and P. Krysinski, *Anal. Bioanal. Chem.*, **405**, 3753 (2013).
21. T. Mele, M. Čarman-Kržan and D. M. Jurič, *Int. J. Dev. Neurosci.*, **28**, 13 (2010).
22. H. Lovheim, *Med. Hypotheses*, **78**, 341 (2012).
23. J. W. Mo and B. Ogorevc, *Anal. Chem.*, **73**, 1196 (2001).
24. A. Galvan and T. Wichmann, *Clin. Neurophysiol.*, **119**, 1459 (2008).

25. S. Mohammadi, Mohammad; Akhondzadeh, *Acta Med. Iran.*, **49**, 487 (2011).
26. T. Obata, *J. Neural Transm.*, **109**, 1159 (2002).
27. Y. Song, *Spectrochim. Acta - Part A Mol. Biomol. Spectrosc.*, **67**, 1169 (2007).
28. R. Baron, M. Zayats and I. Willner, *Anal. Chem.*, **77**, 1566 (2005).
29. S. M. Chen and K. T. Peng, *J. Electroanal. Chem.*, **547**, 179 (2003).
30. P. R. Perati, J. Cheng, P. Jandik and V. P. Hanko, *Electroanalysis*, **22**, 325 (2010).
31. J. Chen, J. Zhang, X. Lin, H. Wan and S. Zhang, *Electroanalysis*, **19**, 612 (2007).
32. H. Dong, S. Wang, A. Liu, J. J. Galligan and G. M. Swain, *J. Electroanal. Chem.*, **632**, 20 (2009).
33. T. Łuczak, *Electroanalysis*, **22**, 2641 (2010).
34. H. Yao, S. Li, Y. Tang, Y. Chen, Y. Chen and X. Lin, *Electrochim. Acta*, **54**, 4607 (2009).
35. H. R. Zare and N. Nasirizadeh, *Sensors Actuators, B Chem.*, **143**, 666 (2010).
36. L. Viry, A. Derre, P. Poulin and A. Kuhn, *Phys. Chem. Chem. Phys.*, **12**, 9993 (2010).
37. B. Zeng, Y. Yang and F. Zhao, *Electroanalysis*, **15**, 1054 (2003).
38. M. A. Fotopoulou and P. C. Ioannou, *Anal. Chim. Acta*, **462**, 179 (2002).
39. P. Britz-Mckibbin, J. Wong and D. D. Y. Chen, *J. Chromatogr. A*, **853**, 535 (1999).
40. Y. Su, J. Wang and G. Chen, *Talanta*, **65**, 531 (2005).
41. T. Kamidate, T. Kaide, H. Tani, E. Makino and T. Shibata, *Anal. Sci.*, **17**, 951 (2001).
42. J. Ortiz-Medina, F. Lopez-Urias, H. Terrones, F. J. Rodriguez-Macias, M. Endo and M. Terrones, *J. Phys. Chem. C*, **119**, 13972 (2015).
43. X. Feng, Y. Zhang, J. Zhou, Y. Li, S. Chen, L. Zhang, Y. Ma, L. Wang and X. Yan, *Nanoscale*, **7**, 2427(2015).
44. A. C. R. Fernandez and N. J. Castellani, *ChemPhysChem*, **18**, 2065(2017).
45. A. F. Khan, D. A. C. Brownson, C. W. Foster, G. C. Smith and C. E. Banks, *Analyst*, **142**, 1756 (2017).
46. P. Giannozzi, et. al. *J. Phys. Condens. Matter*, **21**, 395502 (2009).
47. J. D. Head and M. C. Zerner, *Chem. Phys. Lett.*, **122**, 264 (1985).
48. J. P. Perdew, K. Burke and M. Ernzerhof, *Phys. Rev. Lett.*, **77**, 3865 (1996).
49. H. Monkhorst and J. Pack, *Phys. Rev. B*, **13**, 5188 (1976).

50. M. Corno, A. Rimola, V. Bolis and P. Ugliengo, *Phys. Chem. Chem. Phys.*, **12**, 6309 (2010).
51. S. D. Dabhi, B. Roondhe and P. K. Jha, *Phys. Chem. Chem. Phys.*, **20**, 8943 (2018).
52. B. Roondhe, S. D. Dabhi and P. K. Jha, *Appl. Surf. Sci.*, **441**, 588 (2018).
53. S. Grimme, T. O. Chemie and O. I. D. U. Munster, *J. Comput. Chem.*, **27**, 1787 (2006).
54. S. Grimme, J. Antony, S. Ehrlich and H. Krieg, *J. Chem. Phys.*, **132**, 154104 (2010).
55. A. V. Krukau, O. A. Vydrov, A. F. Izmaylov and G. E. Scuseria, *J. Chem. Phys.*, **125**, 224106 (2006).
56. M. J. Frisch, et al., *Gaussian 09 Revis. C.01*, 2010, Gaussian Inc., Wallingford CT.
57. E. C. Anota, Y. Tlapale, M. S. Villanueva and J. A. R. Marquez, *J. Mol. Model.*, **21**, 214 (2015).
58. B. Roondhe, P. K. Jha, *J. Mater. Chem. B*, **6**, 6796 (2018).
59. C.-H. Park and S. G. Louie, *Nano Lett.*, **8**, 2200 (2008).
60. P. Han, K. Akagi, F. Federici Canova, H. Mutoh, S. Shiraki, K. Iwaya, P. S. Weiss, N. Asao and T. Hitosugi, *ACS Nano*, **8**, 9181 (2014).
61. I. Urdaneta, A. Keller, O. Atabek, J. L. Palma, D. Finkelstein-Shapiro, P. Tarakeshwar, V. Mujica and M. Calatayud, *J. Phys. Chem. C*, **118**, 20688 (2014).
62. Sheng S Li, *Semiconductor physical electronics*, Springer Science & Business Media., 2nd edn., 2006.